


# Characteristic length scales from entanglement dynamics in electric-field-driven tight-binding chains

Devendra Singh Bhakuni\* and Auditya Sharma†

*Department of Physics, Indian Institute of Science Education and Research, Bhopal, India*

 (Received 14 May 2018; revised manuscript received 20 June 2018; published 10 July 2018)

We study entanglement dynamics in the nearest-neighbor fermionic chain that is subjected to both dc and ac electric fields. The dynamics gives the well-known Bloch oscillations in the dc field case provided that the system size is larger than the Bloch length, whereas in the ac field case the entropy is bounded and oscillates with the driving frequency at the points of dynamic localization, and has a logarithmic growth at other points. A combined ac+dc field yields super-Bloch oscillations for system sizes larger than the super-Bloch length, which puts a constraint on the device size in a typical nonequilibrium setup to observe super-Bloch oscillations where the device is connected to the leads. Entanglement entropy provides useful signatures for all of these phenomena, and an alternate way to capture the various length scales involved.

DOI: [10.1103/PhysRevB.98.045408](https://doi.org/10.1103/PhysRevB.98.045408)

## I. INTRODUCTION

A charged particle under the influence of a static electric field would be expected to undergo accelerated motion towards infinity. However, in the presence of a periodic lattice potential and electric field, the motion of a quantum particle is oscillatory. These oscillations are known as Bloch oscillations [1–4]. The time period of these oscillations is inversely proportional to the field strength. Although theoretically well understood, Bloch oscillations are hard to control experimentally in normal crystals where lattice imperfections often wash out this effect altogether [5]. However, the advent of semiconductor superlattices, optical lattices, and temperature-tuned waveguides has made it possible to realize Bloch oscillations experimentally [6–10].

The study of Bloch oscillations in a tight-binding framework gives the well-known Wannier-Stark ladder as the energies and Wannier-Stark states as the eigenstates of the Hamiltonian [11]. These states are extended over a length called the *Bloch length*. Hence, to observe Bloch oscillations, the system size must be greater than this length [12]. Also, the equispaced energy spectrum results in the recurrence of any initial state. Thus an initially localized state will again be localized after a Bloch period.

By making the electric field time dependent,  $\mathcal{F}(t) = A \cos \omega t$ , with time period  $T = 2\pi/\omega$ , one would expect that the same periodicity can be seen in the dynamics. However, contrary to this expectation, only at certain special ratios of the amplitude and the frequency of the drive can the periodicity be seen. This phenomenon is called *dynamic localization* [13–15] and the special ratios are the roots of the Bessel function of order zero.

A more general form of the electric field, which includes both ac and dc fields, gives other interesting effects such as

the *coherent destruction of Wannier-Stark localization* [16,17], which occurs when the dc field is resonantly tuned with the ac drive, and *super-Bloch oscillations* [18–20], which occur for slight detuning from the resonant drive. The time period of these oscillations is very large in comparison to Bloch oscillations. Similar to the static field case, a *super-Bloch length* [21,22] is associated with the super-Bloch oscillations, and in order to observe these oscillations, the system size must be greater than this length.

Entanglement [23–25] quantifies the quantum correlations in a state between two parts of a system. In recent times, it has emerged as a unique tool to capture a vast variety of phenomena ranging from quantum phase transitions [26–28], localization/delocalization transitions [29–33], trivial to topological transitions [34–36], etc., in closed systems, to the correlations between a quantum dot and the baths in open quantum systems [37,38].

The entanglement in a Wannier-Stark ladder [39] and various types of quench dynamics has been studied before, both numerically [40,41] and using conformal field theory (CFT) calculations [42]. However, the connection to various phenomena associated with the electric field was not made explicitly. From the time evolution of an initially half-filled state where all the particles are filled in the left half of the chain, we find the appearance of Bloch oscillations and super-Bloch oscillations in the entropy dynamics when the system size is larger than the respective length scales: the Bloch length and super-Bloch length. Hence, a device length greater than the super-Bloch length is required if one has to observe super-Bloch oscillations in a nonequilibrium setup where the device is connected to metallic leads fixed at different chemical potentials and temperatures. Also, oscillatory behavior of the entropy is observed at the dynamically localized point, whereas a logarithmic growth in entropy is seen for the situations where a resonant drive destroys the Wannier-Stark localization.

In this work, we show how a study of entanglement enables the extraction of the various length scales that arise in the dynamics of a tight-binding chain subjected to an electric

\*devendra123@iiserb.ac.in

†auditya@iiserb.ac.in

field. Furthermore, well-known associated phenomena such as Bloch oscillations, dynamic localization, coherent destruction of Wannier-Stark localization, and super-Bloch oscillations are viewed from an entanglement perspective. The organization of this paper is as follows. In the next section, we describe the model Hamiltonian with a general time-dependent field. The subsections present the different forms of the field and the associated phenomena. The following section provides the quench protocol and the entanglement dynamics with numerical results. The summary and conclusions are given in the last section.

## II. MODEL HAMILTONIAN

The Hamiltonian for a one-dimensional (1D) tight-binding model, for a finite system of size  $2L$  sites with electric field, is

$$H = -J \sum_{n=-L+1}^{L-1} c_n^\dagger c_{n+1} + c_{n+1}^\dagger c_n + a\mathcal{F}(t) \times \sum_{n=-L+1}^L (n-1/2)c_n^\dagger c_n, \quad (1)$$

where  $\mathcal{F}(t)$  is the electric field and  $a$  is the lattice parameter. The numerical work is done in units where  $\hbar = 1$ ,  $c = 1$ ,  $e = 1$ ,  $J = 1$ ,  $a = 1$  (unless otherwise stated). For a constant electric field  $\mathcal{F}(t) = F$ , the dynamics gives the well-known Bloch oscillations, while a sinusoidal driving  $\mathcal{F}(t) = A \cos \omega t$  can give rise to dynamic localization when  $A$  and  $\omega$  are tuned appropriately. In the presence of a combined ac+dc field  $\mathcal{F}(t) = F + A \cos \omega t$ , the phenomenon of coherent destruction of Wannier-Stark localization is seen at resonance, whereas a slight detuning from the resonant condition yields super-Bloch oscillations.

### A. Bloch oscillations

For  $\mathcal{F}(t) = F$ , the exact eigenstates in the  $n \rightarrow \infty$  limit are the Wannier-Stark states,

$$|\Psi_m\rangle = \sum_m \mathcal{J}_{n-m}(2J/aF)|n\rangle. \quad (2)$$

The single-particle energies form a ladder with equal spacing  $E_m = maF$ , where  $m = 0, \pm 1, \pm 2, \dots$ . However, for finite system sizes one observes nonlinear behavior at the ends of the spectrum—these end effects are diminished on increasing system size.

A natural length scale of the problem is the Bloch length [11],

$$L_B = \frac{4J}{F}. \quad (3)$$

One can observe Bloch oscillations with the frequency  $\omega_B = aF/\hbar$  in the dynamics if the system size is greater than the Bloch length. This can be easily seen by studying the time evolution of the mean square single-particle width,

$$\sigma^2(t) = \langle n^2(t) \rangle - \langle n(t) \rangle^2, \quad (4)$$

when the initial state is a single particle localized at the center of the chain. The time evolution for a time equal to an integer multiple of  $T_B$  must return the system back to where it started,

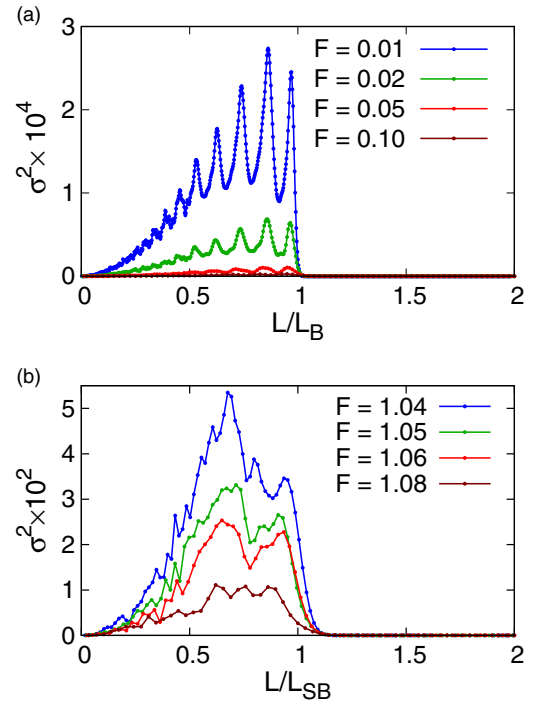


FIG. 1. Mean square single-particle width of the wave packet at  $t = 5T_B$  (top) and  $t = 2T_{SB}$  (bottom) as a function of system size rescaled to Bloch length and super-Bloch length, respectively. The transition shows the requirement of a device size greater than Bloch length and super-Bloch length to observe the oscillations. (Parameters:  $A = 2.0$  and  $\omega = 1.0$ .)

if Bloch oscillations are present. Figure 1(a) shows the mean square width of the wave packet calculated for different field strengths at a time which is an integer multiple of  $T_B$  (we show data for the specific case of  $5T_B$ ), as a function of the system size rescaled by the Bloch length. Since the initial state is a localized state with  $\sigma^2 = 0$  and the same state will reappear after a Bloch period (see Supplemental Material [49] for more information), the mean square width at  $t = nT_B$  should also go to zero. However, this happens only when the system size is larger than the Bloch length.

### B. Dynamic localization

For a time-dependent electric field, the solution of the time-dependent Schrödinger equation for the Hamiltonian  $H$  is given by the Houston states or accelerated Bloch states [14,43] as

$$|\psi_k(t)\rangle = \exp\left(-\frac{i}{\hbar} \int_0^t E[q_k(\tau)]d\tau\right) \sum_n |n\rangle \exp[inq_k(t)a], \quad (5)$$

where the quasimomentum's time dependence can be obtained from the equation of motion as

$$q_k(t) = k + \frac{1}{\hbar} \int_0^t d\tau \mathcal{F}(\tau). \quad (6)$$

The dispersion  $E(q_k) \equiv -2J \cos(q_k a)$  is that of the nearest-neighbor tight-binding model, but with implicit time depen-

dence from the quasimomentum. For a sinusoidal driving  $\mathcal{F}(t) = A \cos(\omega t)$ , the quasimomentum is

$$q_k(t) = k + \frac{A}{\hbar\omega} \sin(\omega t). \quad (7)$$

Although the quasimomentum  $q_k(t)$  is periodic in time with period  $T = 2\pi/\omega$ , the Houston states, however, are *not*  $T$  periodic due to an extra contribution coming from the integral appearing in the exponential. The one cycle average of that contribution is

$$\begin{aligned} \epsilon(k) &= \frac{1}{T} \int_0^T d\tau E[q_k(t)] \\ &= \frac{-2J}{T} \int_0^T d\tau \cos\left(ka + \frac{Aa}{\hbar\omega} \sin(\omega t)\right) \\ &= -2J \mathcal{J}_0\left(\frac{Aa}{\hbar\omega}\right) \cos(ka) \\ &= -2J_{\text{eff}} \cos(ka). \end{aligned} \quad (8)$$

The effect of the drive is thus the well-known renormalization of the hopping parameter. The Houston states can now be decomposed in Floquet notation with the quasienergies  $\epsilon(k)$  as

$$|\psi_k(t)\rangle = |u_k(t)\rangle \exp\left(-\frac{i}{\hbar} \epsilon(k)t\right), \quad (9)$$

where  $|u_k(t)\rangle$  is the  $T$ -periodic function which is obtained by removing the extra contribution term of the exponential.

Hence, the time evolution of any initial state is given by a periodic function  $u_k(t)$  and the phase factors  $\exp[-i\epsilon(k)t/\hbar]$ . However, the phase can be tuned to unity by choosing  $(\frac{Aa}{\hbar\omega})$  to be a zero of the Bessel function of order zero, thereby collapsing the band. In such a scenario, the initial state will reappear after time  $T$  and a localized wave packet remains localized. This phenomenon is known as dynamic localization.

### C. Coherent destruction of Wannier-Stark localization and super-Bloch oscillations

Although a static electric field destroys band formation and leads to Wannier-Stark localization and an ac driving gives dynamic localization, a combination of these two can give rise to the counterintuitive phenomenon of the coherent destruction of Wannier-Stark localization. At resonant tuning, the effective model is the nearest-neighbor tight-binding model, and an initially localized wave packet delocalizes according to the usual mechanism. When a slight detuning from resonance is imposed, super-Bloch oscillations whose frequency is determined by the detuning are seen.

The formalism is the same as given in the previous section, however, the net force is now  $\mathcal{F}(t) = F + A \cos(\omega t)$ . The quasimomentum given by

$$q_k(t) = k + Ft + \frac{A}{\hbar\omega} \sin(\omega t) \quad (10)$$

is *not*  $T$  periodic except at resonance,

$$Fa = n\omega, \quad (11)$$

where  $n$  is an integer;

$$\begin{aligned} q_k(t+T) &= k + \frac{2n\pi}{aT}t + \frac{2n\pi}{a} + \frac{A}{\hbar\omega} \sin(\omega t) \\ &= k + \frac{2n\pi}{aT}t + \frac{A}{\hbar\omega} \sin(\omega t) \\ &= q_k(t), \end{aligned} \quad (12)$$

where the periodicity of the lattice vector is used in the last step. The quasienergies can be calculated as

$$\begin{aligned} \epsilon(k) &= \frac{1}{T} \int_0^T d\tau E[q_k(t)] \\ &= \frac{-2J}{T} \int_0^T d\tau \cos\left(ka + n\omega t + \frac{Aa}{\hbar\omega} \sin(\omega t)\right) \\ &= (-1)^n \mathcal{J}_n\left(\frac{Aa}{\hbar\omega}\right) [-2J \cos(ka)] \\ &= -2J_{\text{eff}} \cos(ka). \end{aligned} \quad (13)$$

It can be seen that ac driving leads to the formation of bands with the hopping parameter getting renormalized. Hence under such a resonant driving the particle can delocalize even though the static electric field is present. However, once again at the zeros of the Bessel function of order  $n$ , there is dynamic localization.

A slight detuning from the resonant drive gives rise to super-Bloch oscillations. The off-drive condition can be written as

$$Fa = (n + \delta)\omega. \quad (14)$$

Under this condition an initially localized wave packet starts oscillating with the time period  $T_{\text{SB}} = \frac{2\pi}{\delta\omega}$  [18,44]. These oscillations are known as super-Bloch oscillations. Similar to the Bloch length, a super-Bloch length is associated with super-Bloch oscillations,

$$L_{\text{SB}} = \frac{J \mathcal{J}_n\left(\frac{Aa}{\hbar\omega}\right)}{\delta\omega}. \quad (15)$$

The super-Bloch oscillations can be seen if the system size is greater than this length. The same is shown in Fig. 1(b) where the wave-packet mean square width is calculated as a function of  $L/L_{\text{SB}}$ .

To summarize this section, we have made a review of the phenomena of Bloch oscillations, dynamic localization, coherent destruction of Wannier-Stark localization, and super-Bloch oscillations. We have shown how the length scales  $L_B$  and  $L_{\text{SB}}$  can be extracted from a study of wave-packet width. This section sets the scene for how these phenomena may be viewed from an entanglement perspective in the next section.

## III. ENTANGLEMENT ENTROPY AND QUENCH DYNAMICS

Quantum entanglement quantifies the lack of information of any subsystem despite full knowledge of the overall system, and is also a measure of how one part of the system is correlated with another part. Although various measures of entanglement are available in the literature [37,45–47], the one that is most widely used as an entanglement measure is the von Neumann entropy.

Let  $\rho$  be the density matrix which describes the full state of the system. The von Neumann entropy of the any subsystem  $A$  is defined as

$$S_A = -\text{Tr}(\rho_A \log \rho_A), \quad (16)$$

where  $\rho_A$  is the reduced density matrix of subsystem  $A$ , i.e.,  $\rho_A = \text{Tr}_B(\rho)$ , with  $\text{Tr}_B$  denoting the partial trace with respect to subsystem  $B$ . When the overall state  $\rho$  is pure, the von Neumann entropy  $S_A$  is also the entanglement entropy between  $A$  and  $B$ .

In a noninteracting quadratic fermionic system, the von Neumann entropy can be directly computed from the two-point correlation matrix [48] of the subsystem  $A$ :  $C_{mn} = \langle c_m^\dagger c_n \rangle$ . The von Neumann entropy is given in terms of the eigenvalues  $n_\alpha$  of the subsystem correlation matrix as

$$S = \sum_{\alpha} [-(1 - n_{\alpha}) \ln(1 - n_{\alpha}) - n_{\alpha} \ln n_{\alpha}]. \quad (17)$$

A generalization of the above result facilitates the study of the dynamics of entanglement. The system is initially prepared in the ground state of an unperturbed Hamiltonian and then suddenly a suitable quenching Hamiltonian is switched on, and the resulting time evolution governed by the new Hamiltonian is tracked. The time-dependent correlation matrix is then directly constructed from the time evolution of the state. Finally, from the time-dependent eigenvalues of the subsystem correlation matrix, we have access to the dynamics of entanglement entropy.

The time evolution of the initial state is given by

$$|\psi(t)\rangle = e^{-iHt/\hbar} |\psi(0)\rangle. \quad (18)$$

The time-dependent correlation matrix can be written as

$$C_{mn}(t) = \langle \psi(t) | c_m^\dagger c_n | \psi(t) \rangle = \langle \psi_0 | c_m^\dagger(t) c_n(t) | \psi_0 \rangle, \quad (19)$$

where we have switched to the Heisenberg picture. Using the time evolution of fermionic operators  $c_j^\dagger$  and  $c_j$ , we can simplify the expression for the correlation matrix as (see Supplemental Material [49] for more information)

$$C(t) = U^\dagger(t) C(0) U(t), \quad (20)$$

where  $U_{jk}(t) = \sum_n D_{jn}^* \exp(-i\epsilon_n t/\hbar) D_{nk}$  and the matrix  $D$  diagonalizes the new Hamiltonian.

In a quenching protocol, where the final Hamiltonian includes a static electric field, the form of the unitary matrix  $U$  can be written as [11]

$$U_{nn'}(t) = \mathcal{J}_{n-n'} \left( \frac{4J}{\hbar\omega_B} \sin \frac{\omega_B t}{2} \right) e^{i(n-n')(\pi - \omega_B t)/2 - in'\omega_B t}. \quad (21)$$

Since  $U(t)$  is periodic in time with the Bloch period, the correlation matrix also follows the same periodicity. Now, the correlation matrix can be written as

$$\begin{aligned} C_{mn} &= \sum_{qq'} \mathcal{J}_{q-m} \left( \frac{4J}{\hbar\omega_B} \sin \frac{\omega_B t}{2} \right) e^{-i(q-m)(\pi - \omega_B t)/2 + im\omega_B t} \\ &\times C_{qq'}(0) \mathcal{J}_{q'-n} \left( \frac{4J}{\hbar\omega_B} \sin \frac{\omega_B t}{2} \right) \\ &\times e^{-i(q'-n)(\pi - \omega_B t)/2 - in\omega_B t}, \end{aligned}$$

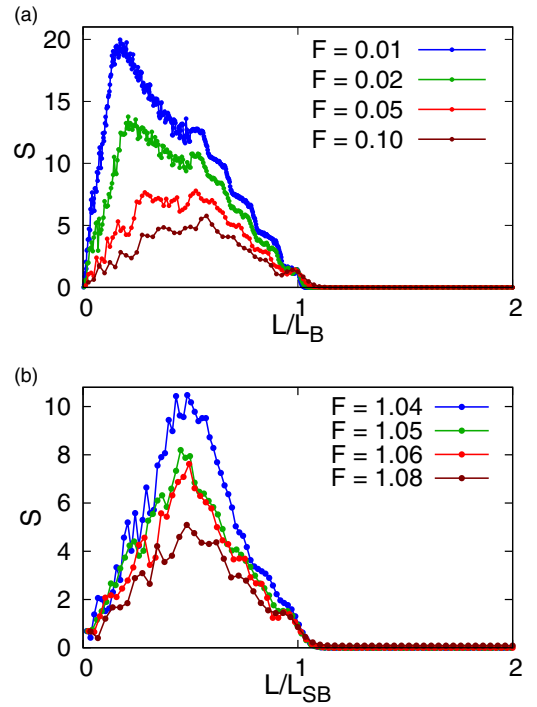


FIG. 2. Entanglement entropy as a function of  $L/L_B$  and  $L/L_{SB}$  for a dc field (top) and combined ac+dc field with slight detuning (bottom) at  $t = 5T_B$  and  $t = 3T_{SB}$  ( $A = 2.0$  and  $\omega = 1.0$ ). The initial state is a half-filled state where all the particles are filled on the left half of the chain. The entropy becomes zero when the system size is larger than the Bloch length and super-Bloch length, respectively.

which, in conjunction with Eq. (17), yields the time-dependent entanglement entropy. For a time-dependent Hamiltonian, we discretize the time interval into tiny regions where the Hamiltonian does not change appreciably, and the same procedure as above follows within the tiny intervals. In this case, the time evolution operator consists of a series of unitary operators.

The entanglement entropy between the two subsystems for the Wannier-Stark problem was studied in Ref. [39]. The contribution to the entanglement entropy comes from the interface width which is created by the potential gradient. Also, the dynamics after turning off the electric field was studied and a logarithmic growth of the entropy was observed. However, here we entirely focus on the dynamics of the entanglement entropy after the electric field is turned on. The entropy as a function of system size rescaled by the Bloch length and super-Bloch length at  $t = 5T_B$  and  $t = 3T_{SB}$ , respectively, is plotted in Fig. 2. The initial state can be thought of as the ground state of a half-filled nearest-neighbor tight-binding chain with a large electric field, where all the particles are localized to the left of the chain. A transition signifies the minimum system size to observe Bloch oscillations and super-Bloch oscillations. The requirement of a device length larger than the Bloch length has been given in recent work [12], where the device is connected to two metallic leads in a nonequilibrium setting and a transition from a dc regime to a Bloch oscillation regime is observed on varying the device size. Our finding is that a similar result holds

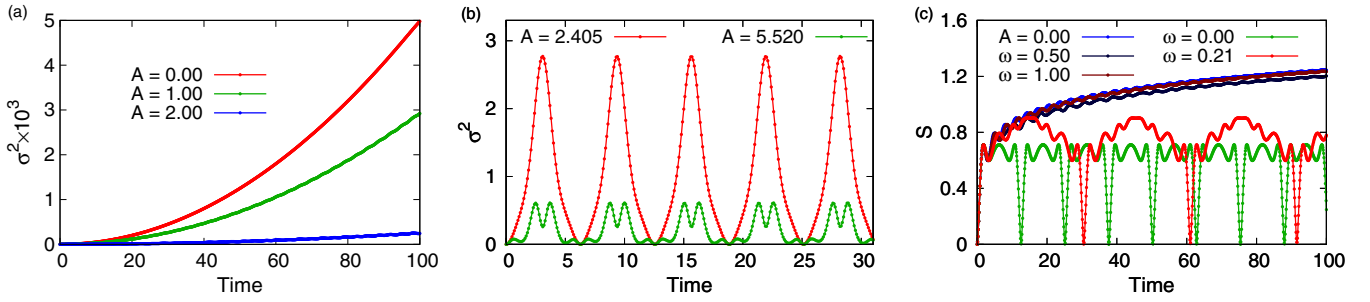


FIG. 3. Mean square width of an initially localized wave packet for an ac driving. Mean square width is unbounded for arbitrary  $A/\omega$  (left), whereas it is bounded and periodic when  $A/\omega$  is a root of the Bessel function of zeroth order (center) (parameters are  $L = 100$  and  $\omega = 1.0$ ). Entanglement entropy (right) for a half-filled localized state. For  $\omega = 0.0$ , the entropy shows Bloch oscillations, whereas for other values the entropy is bounded/unbounded depending on the ratio of  $A/\omega$ . (Parameters are  $L = 100$ ,  $J = 0.5$ , and  $A = 0.5$  for all curves except the blue one.)

for the super-Bloch oscillations in the presence of a combined ac and dc field where the device size has to be greater than the super-Bloch length.

For the case of ac driving, Figs. 3(a) and 3(b) show that the mean square single-particle width of the wave packet is unbounded in time at arbitrary ratios of  $A/\omega$ . In contrast, it remains bounded and oscillatory at the special ratios which are the roots of the Bessel function of order zero. The time evolution of entropy is shown in Fig. 3(c) for various parameters. One can see the Bloch oscillations in the dynamics of entropy for  $\omega = 0.0$  and dynamic localization for the ratio  $A/\omega = 2.405$ , which is a root of the Bessel function of order zero. For all other cases the entropy is unbounded in time, thus signifying delocalization. The coherent destruction of Wannier-Stark localization is shown in Fig. 4(a) for a combined ac and resonantly tuned ac field. The entropy keeps on increasing for a resonantly tuned ac, even in the presence of the dc field. However, again the periodicity of the drive can be seen in the entropy at the special ratios which are now the roots of the Bessel function of order  $n$  [Fig. 4(b)]. Super-Bloch oscillations are observed in the entropy dynamics for the cases of a slight detuning from the resonant condition [Fig. 4(c)]. The chief findings of this section are that entanglement entropy offers a useful alternative perspective for each of the phenomena associated with the application of a general (static or dynamic) electric field.

#### IV. SUMMARY AND CONCLUSIONS

To summarize, we studied the dynamics of many-body entanglement in a nearest-neighbor tight-binding chain with different forms of the electric field. For the static electric field we find that the dynamics captures the well-known Bloch oscillations with the constraint that the system size must be greater than the Bloch length. A system size scaling of the entanglement entropy at  $t = nT_B$  shows a transition from a dc regime to Bloch oscillation regime. For an ac field we find that the entropy oscillates with the driving frequency at the dynamically localized point, whereas at other points it is unbounded. For a combined ac+dc form of the field we find that at a resonantly tuned dc field, the unboundedness of entanglement entropy verifies the coherent destruction of the localization caused by the dc field, whereas a slight detuning from the resonance condition leads to super-Bloch oscillations in the entropy dynamics. From the system size scaling of the super-Bloch oscillations, we find a transition from the dc regime to the super-Bloch oscillation regime which demands a minimum system size to observe super-Bloch oscillations.

Our results in a closed system suggest that if one has to study super-Bloch oscillations in an open system which includes a setup where a device is coupled to the metallic leads, the device size has to be greater than the super-Bloch length to observe super-Bloch oscillations. We believe that the same experimental setup, as put forward in Ref. [12], can

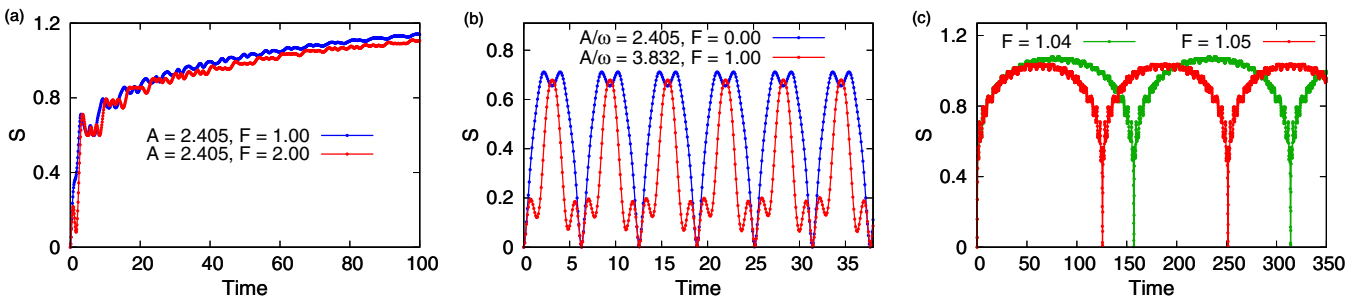


FIG. 4. Destruction of Wannier-Stark localization (left) for resonantly tuned driving  $F = n\omega$ ,  $n = 1, 2, \dots$ , and dynamic localization (center) under the action of both static electric field and ac driving from the dynamics of entanglement entropy. Super-Bloch oscillations captured by entanglement entropy for a detuning from the resonant driving (right). The parameters are  $L = 100$  for all plots  $J = 0.5$  for (a), (b) and  $A = 3.0$ ,  $J = 0.5$  for (c).

be generalized for this purpose. Furthermore, time-dependent phenomena in a nonequilibrium setup have mostly been studied with a small number of degrees of freedom (such as a quantum dot, for example). Therefore, it would be interesting to build on our current work and extend it to study nonequilibrium properties of the nearest-neighbor chain that is subjected to a time-dependent electric field.

## ACKNOWLEDGMENTS

We thank Vikram Tripathi for useful discussions. A.S. is grateful to SERB for the startup grant (File No. YSS/2015/001696). D.S.B. acknowledges support from the University Grants Commission (UGC), India for his Ph.D. fellowship.

- 
- [1] C. Zener, *Proc. R. Soc. London, Ser. A* **145**, 523 (1934).  
 [2] G. H. Wannier, *Phys. Rev.* **117**, 432 (1960).  
 [3] J. B. Krieger and G. J. Iafrate, *Phys. Rev. B* **33**, 5494 (1986).  
 [4] A. M. Bouchard and M. Luban, *Phys. Rev. B* **52**, 5105 (1995).  
 [5] P. Hofmann, *Solid State Physics: An Introduction* (Wiley, Hoboken, NJ, 2015).  
 [6] E. E. Mendez and G. Bastard, *Phys. Today* **46**(6), 34 (1993).  
 [7] C. Waschke, H. Roskos, K. Leo, H. Kurz, and K. Kohler, *Semicond. Sci. Technol.* **9**, 416 (1994).  
 [8] T. Dekorsy, P. Leisching, C. Waschke, K. Kohler, K. Leo, H. Roskos, and H. Kurz, *Semicond. Sci. Technol.* **9**, 1959 (1994).  
 [9] M. Ben Dahan, E. Peik, J. Reichel, Y. Castin, and C. Salomon, *Phys. Rev. Lett.* **76**, 4508 (1996).  
 [10] O. Morsch, J. H. Müller, M. Cristiani, D. Ciampini, and E. Arimondo, *Phys. Rev. Lett.* **87**, 140402 (2001).  
 [11] T. Hartmann, F. Keck, H. Korsch, and S. Mossmann, *New J. Phys.* **6**, 2 (2004).  
 [12] B. S. Popescu and A. Croy, *Phys. Rev. B* **95**, 235433 (2017).  
 [13] D. H. Dunlap and V. M. Kenkre, *Phys. Rev. B* **34**, 3625 (1986).  
 [14] S. Arlinghaus, M. Langemeyer, and M. Holthaus, *Dynamical Tunneling: Theory and Experiment* (2011), p. 289.  
 [15] A. Eckardt, M. Holthaus, H. Lignier, A. Zenesini, D. Ciampini, O. Morsch, and E. Arimondo, *Phys. Rev. A* **79**, 013611 (2009).  
 [16] M. Holthaus, G. Ristow, and D. Hone, *Europhys. Lett.* **32**, 241 (1995).  
 [17] M. Holthaus, G. H. Ristow, and D. W. Hone, *Phys. Rev. Lett.* **75**, 3914 (1995).  
 [18] K. Kudo and T. S. Monteiro, *Phys. Rev. A* **83**, 053627 (2011).  
 [19] A. R. Kolovsky, *J. Sib. Fed. Univ., Math. Phys.* **3**, 311 (2010).  
 [20] R. Caetano and M. Lyra, *Phys. Lett. A* **375**, 2770 (2011).  
 [21] W. Hu, L. Jin, and Z. Song, *Quantum Inf. Process.* **12**, 3569 (2013).  
 [22] E. Haller, R. Hart, M. J. Mark, J. G. Danzl, L. Reichsöllner, and H.-C. Nägerl, *Phys. Rev. Lett.* **104**, 200403 (2010).  
 [23] N. Laflorencie, *Phys. Rep.* **646**, 1 (2016).  
 [24] L. Amico, R. Fazio, A. Osterloh, and V. Vedral, *Rev. Mod. Phys.* **80**, 517 (2008).  
 [25] I. Peschel and V. Eisler, *J. Phys. A* **42**, 504003 (2009).  
 [26] T. J. Osborne and M. A. Nielsen, *Phys. Rev. A* **66**, 032110 (2002).  
 [27] A. Osterloh, L. Amico, G. Falci, and R. Fazio, *Nature (London)* **416**, 608 (2002).  
 [28] G. Vidal, J. I. Latorre, E. Rico, and A. Kitaev, *Phys. Rev. Lett.* **90**, 227902 (2003).  
 [29] N. Roy and A. Sharma, *Phys. Rev. B* **97**, 125116 (2018).  
 [30] G. Roósz, U. Divakaran, H. Rieger, and F. Iglói, *Phys. Rev. B* **90**, 184202 (2014).  
 [31] S. Bera, H. Schomerus, F. Heidrich-Meisner, and J. H. Bardarson, *Phys. Rev. Lett.* **115**, 046603 (2015).  
 [32] M. Serbyn, Z. Papić, and D. A. Abanin, *Phys. Rev. Lett.* **110**, 260601 (2013).  
 [33] J. H. Bardarson, F. Pollmann, and J. E. Moore, *Phys. Rev. Lett.* **109**, 017202 (2012).  
 [34] R. Nehra, D. S. Bhakuni, S. Gangadharaiah, and A. Sharma, [arXiv:1803.00569](https://arxiv.org/abs/1803.00569) [Phys. Rev. B (to be published)].  
 [35] J. Sirker, M. Maiti, N. Konstantinidis, and N. Sedlmayr, *J. Stat. Mech.: Theory Exp.* (2014) P10032.  
 [36] J. Cho and K. W. Kim, *Sci. Rep.* **7**, 2745 (2017).  
 [37] A. Sharma and E. Rabani, *Phys. Rev. B* **91**, 085121 (2015).  
 [38] H. S. Sable, D. S. Bhakuni, and A. Sharma, *J. Phys.: Conf. Ser.* **964**, 012007 (2018).  
 [39] V. Eisler, F. Iglói, and I. Peschel, *J. Stat. Mech.: Theory Exp.* (2009) P02011.  
 [40] V. Eisler and I. Peschel, *Ann. Phys.* **17**, 410 (2008).  
 [41] V. Eisler and I. Peschel, *J. Stat. Mech.: Theory Exp.* (2007) P06005.  
 [42] P. Calabrese and J. Cardy, *J. Stat. Mech.: Theory Exp.* (2007) P10004.  
 [43] W. Houston, *Phys. Rev.* **57**, 184 (1940).  
 [44] S. Longhi and G. Della Valle, *Phys. Rev. B* **86**, 075143 (2012).  
 [45] J. Eisert, M. Cramer, and M. B. Plenio, *Rev. Mod. Phys.* **82**, 277 (2010).  
 [46] G. Vidal and R. F. Werner, *Phys. Rev. A* **65**, 032314 (2002).  
 [47] W. K. Wootters, *Phys. Rev. Lett.* **80**, 2245 (1998).  
 [48] I. Peschel, *J. Phys. A: Mathematical and General* **36**, L205 (2003).  
 [49] See Supplemental Material at <http://link.aps.org/supplemental/10.1103/PhysRevB.98.045408> for detailed description of the time-evolution of the state, and the correlation matrix approach to compute entanglement.